POLITECNICO DI TORINO
Repository ISTITUZIONALE

Modeling of Exposure to Low-Frequency Electromagnetic Fields of Workers in Arbitrary Posture

Original
Modeling of Exposure to Low-Frequency Electromagnetic Fields of Workers in Arbitrary Posture / Conchin Gubernati, A., Freschi, F., Giaccone, L., Scorretti, R., Seppecher, L., Vial, G.. - In: IEEE TRANSACTIONS ON MAGNETICS. - ISSN 0018-9464. - ELETTRONICO. - 56:2(2020), pp. 1-4. [10.1109/TMAG.2019.2949391]

Availability:
This version is available at: 11583/2782974 since: 2020-01-22T15:26:02Z

Publisher:
IEEE Magnetics Society

Published
DOI:10.1109/TMAG.2019.2949391

Terms of use:

This article is made available under terms and conditions as specified in the corresponding bibliographic description in the repository

Publisher copyright

(Article begins on next page)

20 November 2026

This article has been accepted for inclusion in a future issue of this journal. Content is final as presented, with the exception of pagination.

Modeling of Exposure to Low-Frequency Electromagnetic Fields of Workers in Arbitrary Posture

Alice Conchin Gubernati [1], Fabio Freschi [1], Luca Giaccone [1], Riccardo Scorretti [2], Laurent Seppecher[3], and Grégory Vial [3]

[1]Dipartimento Energia "G. Ferraris," Politecnico di Torino, 10129 Torino, Italy
[2]Univ Lyon, Université Claude Bernard Lyon 1, INSA Lyon, EC Lyon, CNRS, Ampére, 69100 Villeurbanne, France
[3]Univ Lyon, École centrale de Lyon, CNRS UMR 5208, Institut Camille Jordan, F-69134 Écully, France

At the present time, numerical dosimetry has reached a certain level of maturity and dedicated commercial software packages are already available. However, the fast and accurate characterization of exposure in real conditions is still challenging for many reasons. For instance, when the exact body posture has to be considered, the classical approach is to evaluate the source magnetic field and then to perform a dosimetric computation with a postured phantom. We propose a different approach that, thanks to a change of variable, makes it possible to use a non-postured body model by deforming the source term. We show that for some rigid transformations, this procedure does not end up in a change of tissue conductivity, which is localized in knees, elbows, and other articulations, where deformations due to posturing are large. Only the source term must be determined by modifying the original one through a suitable transformation.

Index Terms— **Computational phantoms, low-frequency (LF) magnetic fields, numerical dosimetry, posture.**

I. Introduction

EXPOSURE of workers to non-ionizing electromagnetic fields is a source of concern and it is addressed by EU Directives 2013/35/UE [1]. In some cases, mitigation to reduce human exposure to electromagnetic fields is not sufficient (spot welding systems [2], [3]) or even impossible (e.g., MRI systems). In these cases, dosimetric computations are mandatory to assess the respect of the limits. The computational burden of these computations is usually high; moreover, it requires the accurate modeling of the electromagnetic field source and the posture of the exposed worker.

In these years, several realistic and detailed anatomical whole-body models of different types of human beings (e.g., male, female, children, pregnant woman, and so on) have been developed [4]. However, most of them were only available in the standing position with their arms along their sides. This greatly limited the possibility of studying the electromagnetic safety in realistic exposure situations. For this reason, postured phantoms based on the models with the upright configuration started to be developed such as the sitting one [5] or the one with outstretched arms [6]. Posture transformations are based on maintaining internal tissues and organ continuity. Some methods to posture existing phantoms have been developed, such as those in [7], where a procedure for the posture transformation of the anatomically realistic whole-body models has been proposed and a software package to construct an arbitrary posture model has been created. These postured phantoms allowed carrying out the evaluation of human exposure to electromagnetic fields in realistic scenarios. However, posturing computational phantoms is a cumbersome task [7], [8], which necessarily introduces some approximations.

The purpose of this article is to show that, from a numerical point of view, the evaluation of human exposure to low-frequency (LF) electromagnetic fields can avoid a postured phantom. We propose a completely different approach based on an equivalent deformation of the source term, which allows performing all dosimetric computations on a non-postured phantom, maintaining the same level of approximation of the postured model.

Manuscript received August 16, 2019; revised September 29, 2019; accepted October 18, 2019. Date of current version January 20, 2020. Corresponding author: A. Conchin Gubernati (e-mail: alice.conchin@polito.it).

Color versions of one or more of the figures in this article are available online at http://ieeexplore.ieee.org.

Digital Object Identifier 10.1109/TMAG.2019.2949391

II. Methods

Geometric transformations are well known in computational electromagnetics [9], [10]. In general, a change of variable leads to a fictitious modification of material properties, which depends on the Jacobian matrix of the transformation. In this section, the differences between the classical approach and the proposed one are highlighted. In particular, we focus on the role played by the Jacobian matrix in the considered transformations.

A. Classical Approach

As underlined in Section I, in the classical approach the phantom assumes the required posture to reproduce a real scenario. Since in the LF numerical dosimetry the induced currents into the human body are too weak to modify the source field, human exposure to electromagnetic field problems can be solved by using the finite integration technique (FIT) using the electric scalar potential as unknown. This method can be seen as the extension of the scalar potential finite difference to tetrahedral meshes [11]. In the algebraic framework, the linear system is

$$\mathbf{G}^{\mathrm{T}}\mathbf{M}_{\sigma}\mathbf{G}\boldsymbol{\varphi} = -j\omega\mathbf{G}^{\mathrm{T}}\mathbf{M}_{\sigma}\mathbf{a} \tag{1}$$

where $\mathbf{G}$ is the edge-to-node incidence matrix, $\mathbf{M}_\sigma$ is the conductance matrix, $\boldsymbol{\varphi}$ is the electric scalar potential, and $\mathbf{a}$ is the line integral of the magnetic vector potential due to the sources along the mesh edges [12] (the bold letters will indicate the matrices and the vectors throughout this article).

The right-hand side of (1) can be also evaluated knowing only the magnetic flux density (e.g., measurements). Details about solving this type of problem can be found in [13].

B. Proposed Method

Since in the proposed method the phantom is non-postured, formulation (1) must be rewritten by considering a new tissue conductivity and a new source term. Let us assume that the map $f : \Omega \mapsto \Omega_p$ takes the non-postured body Ω to the postured one Ω_p. Hereafter, the subscript p indicates the quantities that depend explicitly on the posture of the body. Formulation (1) can be rewritten as

$$\mathbf{G}^{\mathrm{T}}\mathbf{M}_{\sigma_p}\mathbf{G}\boldsymbol{\varphi} = -j\omega\mathbf{G}^{\mathrm{T}}\mathbf{M}_{\sigma_p}\mathbf{a}_p. \tag{2}$$

This change of variable simplifies computations because now (2) refers directly to the non-postured body, eliminating the posturing step. On the other hand, elements dependent on the effect of the posture, i.e., tissue conductivity tensor $\mathbf{M}_{\sigma_p}$ and the source term $\mathbf{a}_p$, must be determined [10]. Both quantities depend on the Jacobian matrix $\mathbf{J}_p$ of the map f

$$\mathbf{M}^{\mathrm{loc}}_{\sigma_p} = \mathbf{J}_p^{-1}\mathbf{M}^{\mathrm{loc}}_{\sigma}\mathbf{J}_p^{-\mathrm{T}} \cdot |\mathbf{J}_p|; \quad \mathbf{a}_p = \mathbf{J}_p^{\mathrm{T}}\mathbf{a}. \tag{3}$$

It is important to underline that $\mathbf{M}^{\mathrm{loc}}_{\sigma_p}$ is locally computed and then the domain-based matrix $\mathbf{M}_{\sigma_p}$ is assembled in a classical fem-like fashion. The Jacobian matrix is linked to the applied transformation.

C. Human Body Transformations

Movements that a human body can perform are manifold: flexion, extension, rotation, abduction, adduction, and circumduction. They have to be reproduced using geometric transformations when the postured phantom is created. The geometric transformations that can be used are translation, rotation, and stretching.

Translation and rotation belong to the isometry group, i.e., they are distance-preserving transformations between metric spaces. In particular, the Jacobian matrix of translation is the identity matrix. This means that, in (3), it does not contribute and, so, the tissue conductivity matrix can be rewritten as

$$\mathbf{M}^{\mathrm{loc}}_{\sigma_p} = \mathbf{M}^{\mathrm{loc}}_{\sigma}.$$

Instead, since rotation is a direct isometry, its Jacobian matrix is orthogonal, i.e., $\mathbf{J}_p^{\mathrm{T}} = \mathbf{J}_p^{-1}$, and $|\mathbf{J}_p| = 1$. In most practical cases, the local conductivity is isotropic, so $\mathbf{M}^{\mathrm{loc}}_{\sigma} = \sigma\mathbf{I}$. For this reason, the tissue conductivity tensor described in (3) can be rewritten as

$$\begin{aligned}\mathbf{M}^{\mathrm{loc}}_{\sigma_p} &= \mathbf{J}_p^{-1}\mathbf{M}^{\mathrm{loc}}_{\sigma}\mathbf{J}_p^{-\mathrm{T}} \cdot |\mathbf{J}_p| = \mathbf{J}_p^{\mathrm{T}}\sigma\mathbf{I}\mathbf{J}_p \cdot |\mathbf{J}_p| \\ &= \mathbf{J}_p^{\mathrm{T}}\sigma\mathbf{I}\mathbf{J}_p = \sigma\mathbf{J}_p^{\mathrm{T}}\mathbf{J}_p = \sigma\mathbf{I} = \mathbf{M}^{\mathrm{loc}}_{\sigma}.\end{aligned} \tag{4}$$

Therefore, we can conclude that in the rotation case, the tissue conductivity does not change and only the source term undergoes a transformation.

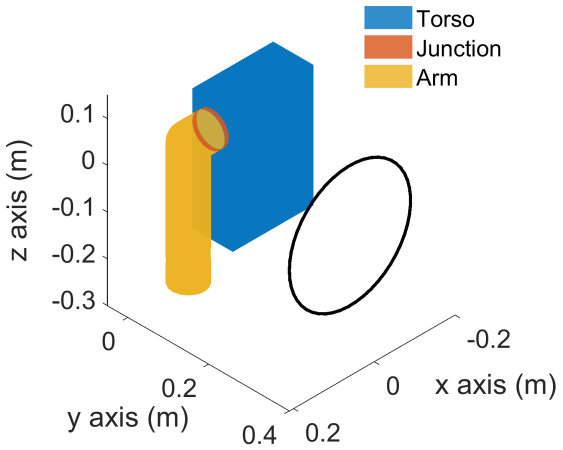


Fig. 1. Exposure scenario in the 3-D domain considered in this article. The three regions (torso, junction zone, and arm) are highlighted by different colors.

Stretching is usually not considered in the posture phantom creation, because much more importance is given to maintain the internal tissues, organ continuity, and mass rather than to introduce physiological concepts, such as muscle contraction. Moreover, stretching produces so small deformations that its transformation matrix is approximately equal to the identity one. In this case, the tissue conductivity matrix becomes

$$\mathbf{M}^{\mathrm{loc}}_{\sigma_p} \simeq \mathbf{M}^{\mathrm{loc}}_{\sigma}.$$

In particular, it can easily be demonstrated that the error has the same order of the stretch factor for small deformations when stretching is along one direction.

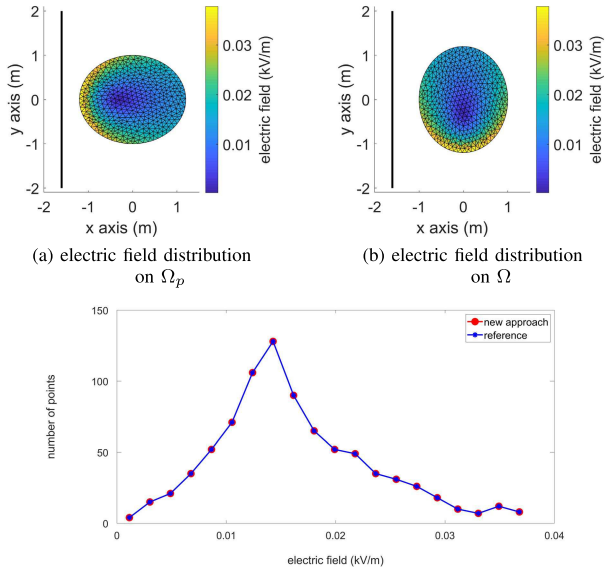
In general, using (2) and (3) instead of (1) simplifies computations to a large extent. The key point is that, in practice, the transformation f can be approximated as a piecewise rigid motion and applied to the source field instead of the computational domain. In fact, when posturing human body, strong deformations are localized in articulations (elbows, knees, and so on): internal organs are only slightly deformed and the brain is not deformed at all. For this reason, we have focused our attention on applying the proposed method to rotation transformation in the 2-D and the 3-D case.

III. Test Cases

The new approach described in Section II is tested on a 2-D and a 3-D domain.

For the sake of simplicity, the 2-D domain Ω consists of an ellipse with center in the origin of the reference system. The minor semi-axis is on the x-axis with length 1 m, while the major semi-axis is on the y-axis and it is 1.2 m long. The tests are performed by considering an infinite vertical wire along y as source field placed at a distance of 1.6 m from the center of the ellipse on the left-hand side. The operating frequency is 50 Hz and the current flowing through the wire is 1 kA.

In the 3-D domain, to compare the *in situ* electric field obtained by using the classical approach and the new one, a simplified phantom exposed to a quasi-static magnetic field is considered. It is composed of three regions (Fig. 1): the

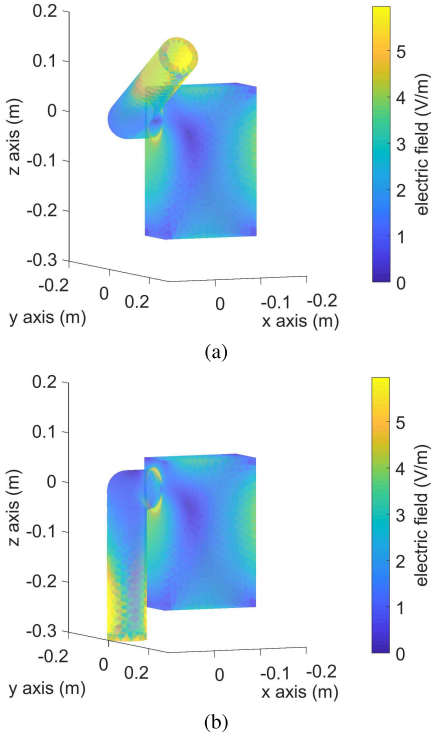


(a) electric field distribution on Ω_p

(b) electric field distribution on Ω

(c) Comparison of induced electric field between the reference case and the proposed method

Fig. 2. (a) Reference solution for the induced electric field. (b) Solution obtained with the proposed method. (c) Electric field frequency diagram for both solutions.



(a)

(b)

Fig. 3. Induced electric field distribution evaluated with (a) the classical approach on the postured phantom and (b) the proposed method on the non-postured phantom.

torso, the arm, and the junction zone, which connects the arm to the torso. The torso is a parallelepiped with dimension $20 \times 10 \times 30$ cm^3, the junction is a cylinder with a 4 cm radius and 1 cm length, and the arm is formed by a cylinder equal to the junction connected to another cylinder with the same radius and 34 cm high. The tissue conductivity σ is 0.2 S/m for each tissue.

A one-loop coil with a radius of 15 cm is located 35 cm from the torso and it is centered in the center of the shoulder. The axis of the coil is the y-axis. The operating frequency is 50 Hz, and the current flowing through the coil is 1 kA.

The tetrahedral mesh in the simplified phantom consists of about 33 000 nodes and 178 000 tetrahedra (divided into about 67 000 in the torso, 64 000 in the junction zone, and 47 000 in the arm). Moreover, the mesh size is 1 mm in the junction zone and 15 mm in the torso and the arm.

IV. Numerical Results

In this section, the numerical results obtained in the 2-D and 3-D domains described in Section III are discussed. The ellipse is rotated clockwise by 90°, and the arm of the 3-D simplified model is rotated by 120° around the x-axis.

A. 2-D Domain

The tests performed on the 2-D domain are based on a 90° clockwise rotation of the ellipse by considering as center of rotation the center of the ellipse.

In the reference case [Fig. 2(a)], the ellipse is 90° rotated and it is evident that the maximum exposure is on the left-hand side, the closest one to the source. Fig. 2(b), instead, shows the induced electric field distribution by using the proposed method. Since in the new approach the domain does not have to be transformed, the ellipse is not 90° rotated. Although the vertical wire is kept in the same position, in Fig. 2(b), the ellipse maximum exposure is on the lower side. This is possible thanks to the transformation of the source term (from $\mathbf{a}$ to $\mathbf{a}_p$) provided in (3). Fig. 2(c) shows the electric field frequency diagram for both methods. It underlines that the results obtained with the proposed method (red curve) are exactly the same as those obtained with the classical approach (blue curve).

B. 3-D Domain

The classical approach (reference case) and the proposed method have been tested on the simple phantom presented in Section III, Fig. 1. As described in Section II-C, the geometric transformation used in the numerical simulations is determined by the rotation angle θ of the Jacobian matrix. In the 3-D domain, it is: 1) equal to zero in the torso (no rotation); 2) equal to $\theta_{\max} = 120°$ in the arm; and 3) linearly increasing in the junction zone, $\theta = \theta_{\max} \cdot (x/x_{\max})$ with $x_{\max} = 1$ cm. This linear variation approximates the real movement of the arm.

Since the axis of the coil passes through the center of the shoulder, the phantom maximum exposure is at the end of the rotated arm, as shown in the reference case in Fig. 3(a). Looking at Fig. 3(b), we can say that the method works as expected, because, if the classic approaches were used, the maximum exposure should be in the center of the shoulder due to the alignment with the coil axis. However, Fig. 3(b) shows that the highest induced electric field concentration is in

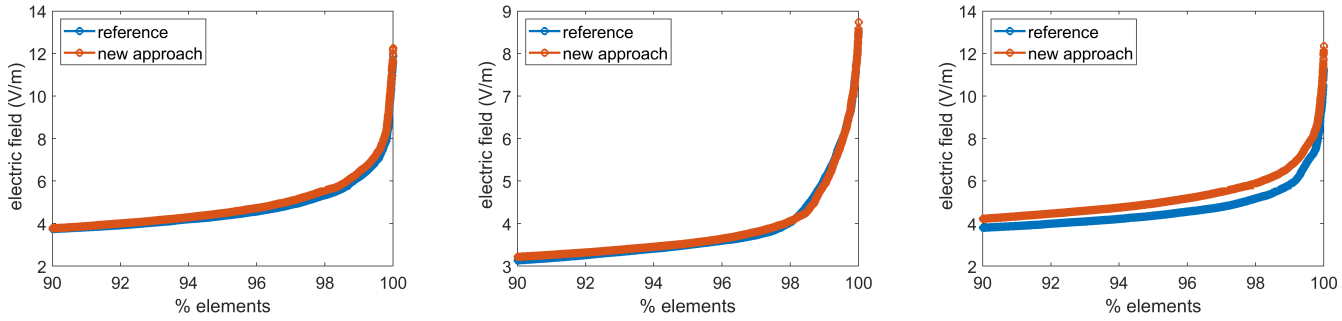


Fig. 4. Comparison of the induced electric field between the two different methods in each component: (a) torso, (b) arm, and (c) junction. Focus between the 90th and the 100th percentile value of the induced electric field.

the arm extremity, exactly as in the reference case [Fig. 3(a)]. Fig. 4 also confirms these results. In fact, paying particular attention between the 90th and the 100th percentile value of the induced electric field (maximum exposure), the results are completely comparable in the torso and in the arm, and there is a little deviation in the junction. The reason is that a complete rotation occurs in the arm, whereas in the junction there is a piecewise rigid motion due to the linear variation of the Jacobian matrix angle. However, the largest deviation in the junction zone, evaluated as the ratio between the induced electric field value computed with the proposed method and the one computed with the classical approach, is $\sim$1.11. It means that there is an overestimation of 11% (more than acceptable in numerical dosimetry).

V. Conclusion

A new approach to perform a dosimetry analysis without a postured body model is proposed. Unlike the classic approach in which all dosimetric computations are performed with a postured phantom, the new method is based on the evaluation of human exposure to electromagnetic fields by using a non-postured domain through a source term transformation.

Among all geometric transformations, rotation best reproduces human body movements. Numerical results in the 2-D and 3-D domains related to this transformation have been reported in Section IV. In the 2-D domain, the results obtained with the proposed method are identical to the reference case. The reason is because rotation is an isometry (rigid transformation) and the use of a simple domain has allowed us not to introduce approximation errors. In the 3-D domain, the numerical results of the induced electric field distribution are comparable in the torso and the arm, while in the junction, there is an overestimation of the 11% between the 90th and the 100th percentile due to the linear variation in the rotation angle. This overestimation is more than acceptable for a dosimetric assessment, since these errors are comparable with the geometric ones due to the posture.

Our next work is to apply the proposed method to a more complicated phantom (e.g., Alvar [14]) in order to validate it.

Acknowledgment

The authors would like to thank the Programme National de Recherche Environnement-Santé-Travail (PNREST) Anses, 2018/1/242, to have funded this project.

References

[1] European Parliament and Council of the European Union, "Directive 2013/35/UE of the European Parliament and of the Council of 26 June 2013 on the minimum health and safety requirements regarding the exposure of workers to the risks arising from physical agents (electromagnetic fields)," Off. J. Eur. Union, L179/1-21, Jun. 2013.

[2] A. Canova, F. Freschi, and L. Giaccone, "How safe are spot welding guns to use?: An analysis of occupational exposure to their magnetic field," *IEEE Ind. Appl. Mag.*, vol. 24, no. 3, pp. 39–47, May/Jun. 2018.

[3] L. Giaccone, V. Cirimele, and A. Canova, "Mitigation solutions for the magnetic field produced by MFDC spot welding guns," *IEEE Trans. Electromagn. Compat.*, to be published.

[4] M.-C. Gosselin *et al.*, "Development of a new generation of high-resolution anatomical models for medical device evaluation: The virtual population 3.0," *Phys. Med. Biol.*, vol. 59, no. 18, pp. 5287–5303, 2014.

[5] T. W. Dawson, K. Caputa, and M. A. Stuchly, "Numerical evaluation of 60 Hz magnetic induction in the human body in complex occupational environments," *Phys. Med. Biol.*, vol. 44, no. 4, pp. 1025–1040, 1999.

[6] T. W. Dawson, K. Caputa, and M. A. Stuchly, "Magnetic field exposures for UK live-line workers," *Phys. Med. Biol.*, vol. 47, no. 7, pp. 995–1012, Apr. 2002.

[7] T. Nagaoka and S. Watanabe, "Postured voxel-based human models for electromagnetic dosimetry," *Phys. Med. Biol.*, vol. 53, no. 24, pp. 7047–7061, Dec. 2008.

[8] J. Gao, "Generation of postured voxel-based human models used for electromagnetic applications," Ph.D. dissertation, Dept. Elect. Eng. Inf. Technol., Technische Univ., Berlin, Germany, 2012.

[9] A. Nicolet, F. Zolla, O. Agha, and S. Guenneau, "Geometrical transformations and equivalent materials in computational electromagnetism," *Int. J. Comput. Math. Elect. Electron. Eng.*, vol. 27, no. 4, pp. 806–819, Jul. 2008.

[10] S. G. Johnson. *Coordinate Transformation and Invariance in Electromagnetism*. Accessed: Oct. 25, 2019. [Online]. Available: https://math.mit.edu/~stevenj/18.369/spring08/coordinate-transform.pdf

[11] T. W. Dawson and M. Stuchly, "Analytic validation of a three-dimensional scalar-potential finite-difference code for low-frequency magnetic induction," *Appl. Comput. Electromagn. Soc. J.*, vol. 11, no. 3, pp. 72–81, 1996.

[12] F. Freschi, L. Giaccone, V. Cirimele, and A. Canova, "Numerical assessment of low-frequency dosimetry from sampled magnetic fields," *Phys. Med. Biol.*, vol. 63, no. 1, 2018, Art. no. 015029.

[13] A. C. Gubernati, F. Freschi, L. Giaccone, T. Campi, V. De Santis, and I. Laakso, "Comparison of numerical techniques for the evaluation of human exposure from measurement data," *IEEE Trans. Mag.*, vol. 55, no. 6, Jun. 2019, Art. no. 5000404.

[14] *Alvar: Adult Whole-Body Anatomic Phantom for Computational Dosimetry*. Accessed: Oct. 25, 2019. [Online]. Available: https://version.aalto.fi/gitlab/ilaakso/alvar